Multidimensional Ablation and Heat Flow during Re-Entry

H. HURWICZ*
Avco Corporation, Wilmington, Mass.

AND

S. FIFER† AND M. KELLY‡
Dian Laboratories, Inc., New York, N. Y.

Two methods of formulating and programing multidimensional ablation problems for electronic analog computation (discrete stepwise ablation and continuous recession) are developed, and two typical solutions are obtained. Savings in required computing equipment and greater ease of computing are achieved by appropriate transformations and/or applications of physically reasonable assumptions. For a composite wing leading edge, it is shown that two-dimensional analysis (compared to one-dimensional) predicts smaller gradients at transitions and lower base temperatures. For an ablative spin-control fin, it is shown that a one-dimensional analysis would have overestimated the complete removal time by approximately $1\frac{1}{2}$ sec out of 32 and would have significantly underestimated the altitude at which stress failure would occur. The choice of the analog-computing method for such design problems is governed by the geometry to be analyzed and the severity of ablation.

Nomenclature

A/A_{ref} = area ratio
c = specific heat
$\delta D/\delta D_{ref}$ = relative dispersion
F = heat of ablation, Eq. (3)
f = internal heat flux, x direction
$\oint$ = vaporization fraction
g = internal heat flux, y direction
H_e/RT_0 = dimensionless enthalpy
h = specific enthalpy of air
h_{v1} = latent heat of vaporization, silica component
h_{v2} = heat of vaporization, reaction, etc., plastic component
k = thermal conductivity
L = slab thickness
n = number of cells
P = fraction of cell ablated, defined following Eq. (17)
p = fixed interface position
Q = $\int qdt$ total heat input
q = external heat flux
R = radius
r,θ = cylindrical coordinates
s = ablation (recession) depth
$\dot{s}$ = ablation (recession) velocity
T = temperature
T^* = temperature; defined in Eq. (19)
$\dot{T}$ = temperature derivative dT/dt
t = time
V/V_{ref} = volumetric ratio
x,y,z = rectangular coordinates
χ = fraction of silica in the reinforced material
α = angle of attack
ϵ = emissivity
η = transpiration coefficient
ρ = density
σ = Stefan-Boltzmann constant
ξ = transformation defined in Eq. (10)
$\xi^{(i)}$ = transformation defined in Eq.(21)
ξ^* = transformation defined in Eq. (20)
θ = angle
ψ_i = $R_0 - s_i - \xi R_i$

Subscripts

A = ablation
$A_{i,j}$ = beginning of ablation of cell i,j
$A1$ = beginning of ablation of cell 1
av = average
b = substructure (or backface of the ablating material)
C = leading edge, spin fin stagnation region
c = cold wall
char = charred material
D = top of the fin
e = outer edge of the boundary layer
i,j,k = interior cell designation in x,y,z directions, respectively
L = leeward direction
m, max = maximum
0 = initial
$P_{i,j}$ = partial ablation of cell i, j
$R_{i,j}$ = end of ablation of cell i,j
$R1$ = end of ablation of cell 1
ref = reference
s = stagnation
ss = steady state
W = windward direction
w = wall, surface
θ = parallel to surface

Introduction

FOR certain areas on entry vehicles, such as ablating leading edges or control surfaces, a one-dimensional analysis of the heat and mass flow is not sufficient. Among the questions that must be answered by two- or three-dimensional analysis are: Do multidimensional fluxes significantly affect temperature response and mass removal, as far as time and amplitude are concerned? Do appreciable lateral flows arise, affecting the structural design? Are the drag, heating, and other aerodynamic performance characteristics changed significantly? Can load failure be more accurately predicted?

The presence of ablation, or surface recession, has been a strong deterrent to multidimensional analysis, because the partial differential equations of heat and mass flow become

* Associate Manager, Engineering Analysis Department, RAD Division. Member AIAA
† President. Member AIAA.
‡ Senior Analyst.

Presented as Preprint 63-180 at the AIAA Summer Meeting, Los Angeles, Calif., June 17–20, 1963; revision received December 13, 1963. This work has been performed under U. S. Air Force Contracts AF33(616)-7483, Materials and Processes Directorate, Aeronautical Systems Division, Wright Patterson Air Force Base, and AF04(647)-258 and AF04(647)-305. The analog computer calculations were performed at Dian Laboratories, Inc., New York, N. Y. The authors wish to acknowledge the assistance of E. Rollo and R. Mascola in the evaluation of the applications.

considerably more complicated. Two-dimensional solutions to the simpler heat-conduction problem exist,[1-4] but the few solutions to problems that involve both heat conduction and mass transfer either assume one-dimensional conduction and restrict the mass transfer to liquid layer flow[5-8] or consider the mass transfer as unidirectional while the heat conduction is treated in two dimensions[9] (similar to one of the solutions presented here). References 10 (Appendix XI) and 11 review the physical considerations attendant to the analysis of multidimensional flow problems and the solutions believed to exist.

The present paper presents two practical schemes for the analog-computer solution of two-dimensional (and possibly three-dimensional) problems involving ablation: one allows for conduction and stepwise ablation, and the other employs a set of shrinking coordinate systems which permits continuous recession of the ablating surface. These methods are then applied to two entry-vehicle problems: a glider wing leading edge, and a spin-control fin.

Mathematical Formulation

The problem of multidimensional ablation and heat flow consists of finding a solution to the heat-conduction equation

$$\rho c(\partial T/\partial t) = \nabla(k\nabla T) \tag{1}$$

in a region R bounded by a moving (ablating) surface $C = C(t)$ on which the normal derivatives are specified. The thermal parameters are generally taken to be constant in what follows. In some cases, a fixed surface temperature T_A may be prescribed at which the material ablates. The right-hand member of Eq. (1) may be expressed in rectangular, cylindrical, or spherical coordinates, and in one, two, or three dimensions. Difference approximations to (1) are usually employed for solution by digital computers, whereas difference-differential approximations are used for analog-computer solutions. The latter are of interest in the present work, which takes advantage of two characteristics of analog computation: simplicity and freedom from stability difficulties. The time variable t is kept continuous, and only the space variables are treated in terms of finite differences. Since time is a continuous variable of the electronic differential analyzer, this computer provides a natural setting for the solution of differential equations.[12]

Three-dimensional ablation problems usually can be reduced to one- or two-dimensional problems by virtue of uniformities characterizing the region R and the boundary conditions defined on C. There is no unique analog-computer method for solving (1) in all generality, but techniques have been developed for various practical small problems. If the problem under consideration can be reduced to, or favorably approximated by, one or some of these cases, the necessary calculations for entry vehicle design can be made.

The heat flux at the front surface prior to ablation is[13]:

$$-k(\partial T/\partial x) = q = q_c[1 - (h_w/h_s)] - \epsilon\sigma T_w^4 \tag{2}$$

where x is measured normal to the surface. When the surface temperature reaches T_A (ablation), Eq. (2) is replaced by

$$-k(\partial T/\partial x) = q - \rho F\dot{s} \tag{3}$$

where $\dot{s}$ is the velocity of surface recession (normal to surface), and F is the heat of ablation.

Difference-differential formulations are presented below for both discrete (stepwise) and continuous recession methods for one- and two-dimensional cases. Each of these two methods for solving ablation problems on analog computers has its strong and weak points. Advantages of the discrete method are: 1) simplicity (a linear conduction problem is solved), and 2) flexibility (various geometries may be approximated by an assembly of cubes with appropriate switching). Disadvantages are: 1) discontinuities are produced by stepwise ablation, and 2) more and more of the computing equipment falls idle as ablated cells are dropped. The continuous recession method produces a continuously moving boundary and smooth temperature-time histories and makes maximum use of computing equipment; however, it is more complex and less flexible, primarily because of the unequal ablation rates for the individual strips being considered.

Stepwise Ablation—One-Dimensional

Let the region $0 \leq x \leq L_0$ be divided into n cells of width Δx, so that $n\Delta x = L_0$. Let x_i be the coordinate of the center of the ith cell, $f_{i-(1/2)}$ the flux entering the cell across the surface with area $\Delta y\Delta z$ at $x = x_i - \Delta x/2$, and $f_{i+(1/2)}$ the corresponding flux leaving the cell at $x_i + \Delta x/2$. Letting $T(x_i,t) = T_i$ represent the average temperature over the width Δx of the ith cell, the heat balance is

$$\Delta x\Delta y\Delta z\rho c\dot{T}_i \equiv \Delta y\Delta z(f_{i-(1/2)} - f_{i+(1/2)}) \tag{4}$$

Approximating the flux terms by

$$\begin{aligned} f_{i-(1/2)} &= k(T_{i-1} - T_i)(\Delta x)^{-1} \\ f_{i+(1/2)} &= k(T_i - T_{i+1})(\Delta x)^{-1} \end{aligned} \tag{5}$$

leads to the standard difference-differential form:

$$\rho c\dot{T}_1 = k(T_{i-1} - 2T_i + T_{i+1})(\Delta x)^{-2} \tag{6}$$

For the first cell,

$$\rho c\dot{T}_1 = (\Delta x)^{-1}[q - k(T_1 - T_2)(\Delta x)^{-1}] \tag{7}$$

For the last cell, the flux at the rear boundary $x = L_0$ is taken to be zero, but there is no prohibition on other boundary conditions.

When $T_1 = T(x_1,t)$ reaches T_A, the entire first cell is assumed to be at T_A. The heat required to ablate the cell is $\Delta x\rho F$ (by definition). If t_{A1} is the time at which T_1 reaches T_A, then the first cell is completely removed by ablation (at time T_{R1}) when

$$\int_{t_{A1}}^{t_{R1}} (q - f_{1/2})dt = \Delta x\rho F \tag{8}$$

The first cell is removed by switching q at time t_{R1} to the face of the second cell and proceeding in a similar manner. For the second cell, Eq. (7) becomes

$$\rho c\dot{T}_2 = (\Delta x)^{-1}[q - k(T_2 - T_3)(\Delta x)^{-1}] \qquad t \geq t_{R1} \tag{9}$$

Continuous Recession—One-Dimensional

A new nondimensional space variable ξ is introduced,[14]

$$\xi = (x - s)/(L_0 - s) \tag{10}$$

which transforms the region $s \leq x \leq L_0$ into the region $0 \leq \xi \leq 1$. The conduction equation becomes

$$\rho c\dot{T}(\xi,t) = \frac{k}{(L_0 - s)^2}\frac{\partial^2 T(\xi,t)}{\partial\xi^2} + \frac{\rho c(1 - \xi)\dot{s}[\partial T(\xi,t)/\partial\xi]}{L_0 - s} \qquad 0 \leq \xi \leq 1 \tag{11}$$

The boundary condition at the receding surface (3) becomes

$$-k\partial T(0,t)/\partial\xi = (L_0 - s)(q - \rho F\dot{s}) \qquad \xi = 0 \tag{12}$$

and at the rear surface, $x = L_0$ (assumed insulated),

$$-k\partial T(1,t)/\partial\xi = 0 \qquad \xi = 1 \tag{13}$$

There are many schemes for replacing (11) by a set of difference-differential equations. One critical check (a necessary but not sufficient condition) is that a steady-state heat balance[14] be satisfied:

$$\int_0^{t_{ss}} qdt = [\rho cs_{ss}T_A] + [\rho Fs_{ss}] + [\rho cL_{ss}T_{ss}] \tag{14}$$

The total heat input equals (heat to raise ablated portion S_{ss} to T_A) plus (heat to ablate S_{ss} at T_A) plus (heat content of remaining slab thickness L_{ss}).

Formulations have been developed[15] for rectangular, cylindrical, and spherical coordinate systems. The correctness of a given formulation can be checked further[14] by considering a semifinite bar and constant q; under these conditions, the recession rate $\dot{s}$ should approach the value $q/(\rho c T_A + \rho F)$ as $t \to \infty$.

Stepwise Ablation—Two-Dimensional

When there is a significant variation in the thermal gradients in two directions, the operator ∇ of (1) must be represented accordingly. An example of such a case is furnished by a rectangularly shaped body in the x-y plane, insulated on three sides and with a q variation in the y direction. For stepwise ablation, the x-y cross section of the body is divided into cells of area $\Delta x \Delta y$. Let f denote the flux in the x direction and g the flux in the y direction. A heat balance for the i,jth cell may be written as

$$\Delta x \Delta y \Delta z \rho c \dot{T}_{i,j} = \Delta y \Delta z (f_{i-(1/2)} - f_{i+(1/2)}) + \Delta x \Delta z (g_{j-\frac{1}{2}} - g_{j+\frac{1}{2}}) \quad (15)$$

Expressing the fluxes in difference form and simplifying gives

$$\rho c \dot{T}_{i,j} = k(T_{i-1,j} - 2T_{i,j} + T_{i+1,j})(\Delta x)^{-2} + k(T_{i,j-1} - 2T_{i,j} + T_{i,j+1})(\Delta y)^{-2} \quad (16)$$

for the interior cells. The equations for the outer cells are expressed in terms of the appropriate boundary conditions. Equation (8) becomes

$$\int_{t_{Ai,j}}^{t_{Ri,j}} [(q - f_{i+(1/2)})\Delta y + (g_{j-\frac{1}{2}} - g_{j+\frac{1}{2}})\Delta x] dt = \Delta x \Delta y \rho F \quad (17)$$

At time $t_{Ri,j}$ the cell is dropped and the boundary condition is applied to the next cell. If the temperature of some specific cell reaches T_A but (17) is never satisfied (ablation stops because of insufficient q), then the fraction P, found by dividing the final value of the left-hand member of (17) by the right-hand member, is taken as a measure of the portion of the cell that has ablated.

Continuous Recession—Two-Dimensional

In a two-dimensional, continuous ablation problem, there is a distinct ablation rate $\dot{s}_j$ for each of the n strips in the y direction and, hence, n transformations of the type (10). Temperature stations that are initially fixed with respect to one another may subsequently depart from one another. It is therefore necessary to perform some sort of interpolation. Figure 1 illustrates an initial alignment a) of temperature stations prior to ablation and a subsequent alignment b). Cell 2,2 is originally adjacent to cell 2,1 and the initial y flux into cell 2,2 from the left is

$$g_{3/2} = k(T_{2,1} - T_{2,2})(\Delta y)^{-1} \quad (18)$$

At the moment illustrated by Fig. 1b, cell 2,2 lies between cells 3,1 and 4,1, so that $T_{2,1}$ in (18) must be replaced by $T_{2,1}{}^*$ which falls between $T_{3,1}$ and $T_{4,1}$ and is found by interpolation:

$$T_{2,1}{}^* = (\xi_{2,1}{}^* - \xi_{3,1})(\Delta\xi)^{-1}(T_{4,1} - T_{3,1}) + T_{3,1} \quad (19)$$

The x coordinate of $T_{2,2}$ at this moment is defined by (10), and since $T_{2,1}{}^*$ has the same x coordinate as $T_{2,2}$,

$$\xi_{2,1}{}^* = \frac{x_{2,2} - s_1}{L_0 - s_1} = \frac{(L_0 - s_2)\xi_{2,2} + s_2 - s_1}{L_0 - s_1} \quad (20)$$

The cell to the right of cell 2,2 is completely ablated. Some approximation must be made to determine the flux across the right-hand boundary of cell 2,2 (e.g., one might assume that the temperature at the right-hand boundary of cell 2,2 has just reached T_A).

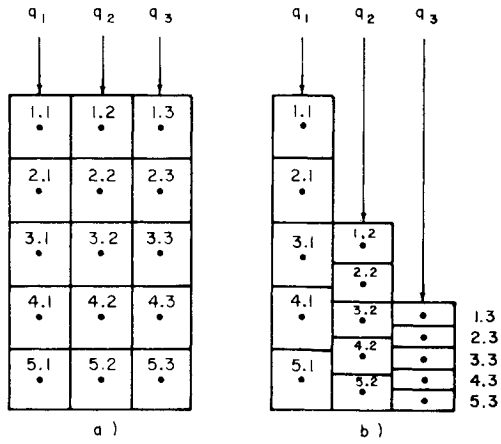

Fig. 1 Two-dimensional finite difference grid for heat conduction and ablation in a moving coordinate system.

For cases of partial ablation, the bar is divided into two regions; the boundary between the ablating and nonablating regions can be fixed in space, at a depth greater by some safe distance than the maximum recession s_m of any strip. In the ablating front region, the standard transformation (10) is used for each ith strip, and, in the rear, the equation of heat flow can be solved in its original linear form in x coordinates, since the interface is fixed.

Applications

Ablation problems generally represent one of three cases: 1) shape change is one-dimensional, but internal heat flow is multidimensional because of the geometrical configuration, 2) shape change is two-dimensional but does not affect the external flow characteristics (it does change internal flow), and 3) two- or three-dimensional shape change produces significant effects on the external as well as internal flows. The selected applications, a wing leading edge and a spin-control fin, are representative of cases 1 and 2, respectively. The spin fin undoubtedly results in case 3 in reality, but effects of external flow are not considered in the present limited study.

Ablation of a Glider Wing Leading Edge

Figure 2 shows the geometry and boundary inputs for a typical glider wing leading edge at 13° angle of attack. The properties of materials used in this calculation are given in Table 1, and the thermal environment parameters q_c and H_e/RT_0 are shown in Fig. 3. The input flux q_c is plotted as a function of time t and angle θ. It is observed that q_c is of long duration, and that its distribution shows a maximum, of course, at the stagnation point $\theta = -13°$ (because $\alpha = +13°$). This is a two-dimensional cylindrical-coordinate problem for most of the ablation region; hence it is possible to use a shrinking-coordinate (radial) system corrected for nonuniformities at the boundaries of the ablation region.

Before solving the two-dimensional problem in its entirety, a set of one-dimensional computations was made to obtain estimates of the ablation depths and temperature gradients in the plastic material. This one-dimensional problem, solved for the various heat inputs around the wing leading edge (Fig. 3), revealed that the maximum ablation depth is approximately 0.2 in. This information served to determine the optimum location of the fixed boundary in the plastic shield of the Fig. 2 model for the two-dimensional analysis.

The transformation for each strip in the ablation section is

$$\xi^{(i)} = (R_0 - r - s_i)/R_i \qquad R_i = R_0 - p - s_i \quad (21)$$

where s_i is the ablation depth of the ith strip. The funda-

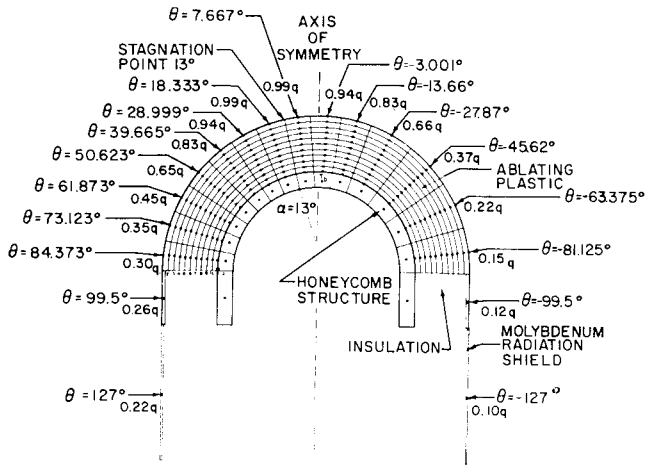

Fig. 2 Analog-computer model and cross-sectional diagram of idealized wing leading edge.

mental equation for the two-dimensional cylindrical-coordinate case is

$$\rho c \frac{\partial T}{\partial t} = \frac{k}{r} \frac{\partial}{\partial r} \left(r \frac{\partial T}{\partial r} \right) + \frac{k}{r^2} \frac{\partial^2 T}{\partial \theta^2} \tag{22}$$

which in the ablation region becomes, with $\psi_i \equiv R_0 - s_i - \xi R_i$,

$$\rho c \frac{\partial T}{\partial t} = \frac{k}{R_i^2} \frac{\partial^2 T}{\partial \xi^2} - \frac{k}{R_i \psi_i} \frac{\partial T}{\partial \xi} + \frac{k}{\psi_i^2} \frac{\partial^2 T}{\partial \theta^2} + \rho c \frac{\dot{s}_i}{R_i} (1 - \xi^{(i)}) \frac{\partial T}{\partial \xi} \tag{23}$$

The boundary condition (3) in cylindrical coordinates is

$$k(\partial T/\partial r) = q_i - \rho F \dot{s}_i \tag{24}$$

where

$$F = h_{v_2} + \eta(h_s - h_w) \tag{25}$$

for the material under consideration. By transformation of (21), Eq. (24) becomes

$$k(\partial T/\partial \xi) = R_i q_i - \rho F R_i \dot{s}_i \tag{26}$$

Many techniques exist for forming finite-difference approximations to the space derivatives of (23) and for inserting the boundary condition (26). Purely formal approaches, however, can result in invalid formulations. For example, (23) may be written as

$$\rho c \frac{\partial T}{\partial t} = \frac{k}{R_i^2 \psi_i} \frac{\partial}{\partial \xi} \left(\psi_i \frac{\partial T}{\partial \xi} \right) + \frac{k}{\psi_i^2} \frac{\partial^2 T}{\partial \theta^2} + \rho c \frac{\dot{s}_i}{R_i} (1 - \xi^{(i)}) \frac{\partial T}{\partial \xi} \tag{27}$$

For boundary cells, it would seem mathematically proper to insert the right-hand member of (26) into (27) for the corresponding $k\partial T/\partial \xi$ term. It can be shown that such a formal substitution does not produce a steady-state heat balance, because not every term containing the expression $\partial T/\partial \xi$ in (27) is a genuine flux term. Specifically, the last term in the equation is a convection term due to the introduction of moving coordinates. The first term in the right-hand member is the only one to which the boundary condition is applied, because it is the only one involving fluxes in the ξ direction.

Figure 4 shows that, in the region of the interface between the plastic heat shield and the molybdenum skin, the one-dimensional analysis indicates large transitions because of the mismatch of the emissivities, $\epsilon = 0.7$ for the plastic and $\epsilon_{MO} = 0.2$ for the uncoated molybdenum (a somewhat extreme case). The two-dimensional calculations produce a smoothed curve of temperature in that region. The two-dimensional solution for the coated molybdenum ($\epsilon_{MO} = 0.7$) shows a very small gradient at the interface. It can be seen that the one-dimensional analysis overestimated the base temperature T_b by 50°–70°F (at ~ 1100°F) in the stagnation region.

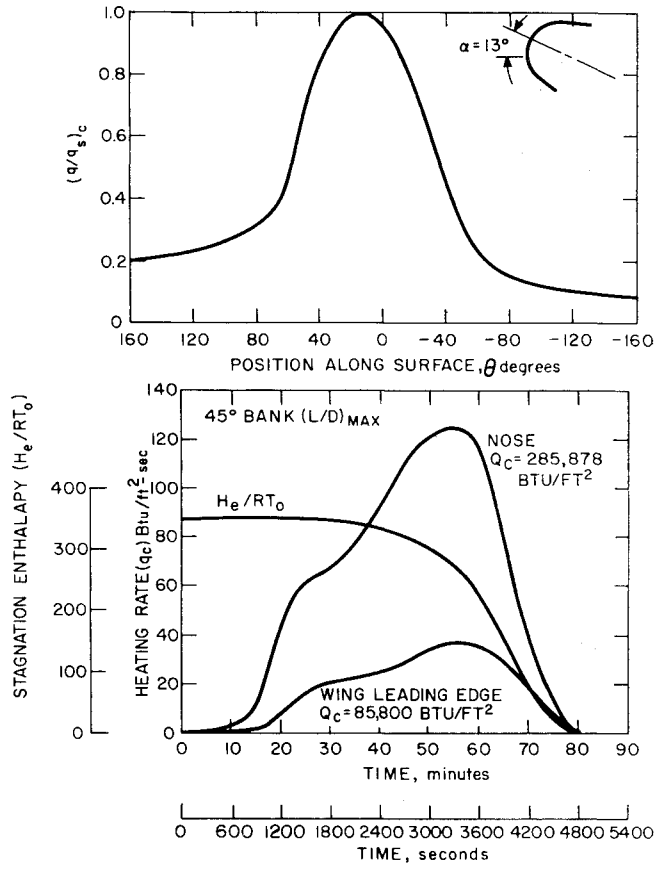

Fig. 3 Typical glide re-entry vehicle aerothermal environment.

The total amount of material ablated is small and virtually unaffected by two-dimensional heat flow in the plastic shield; the contour of the heating is not changed enough to change the aerothermodynamic environment significantly. The region ablated and the post-ablation isotherms are presented in Fig. 5. Temperature gradients in the honeycomb structure normal to its surface are not excessive. The longitudinal gradients are less severe than those a purely one-dimensional computation would have given. This analysis demonstrates that the thermal effect of the substructure for a glider vehicle

Table 1 Properties of materials used in two-dimensional thermal analysis of a wing leading edge

Material	ρ, lb/ft³	c, Btu/lb-°F	k, Btu/hr-ft-°F	ϵ
Heat shield (X-3000 plastic)[a]	72	0.30	0.10	0.7
Radiation shield (molybdenum)	634	0.065	80.00	0.2 0.7
Metallic honeycomb structure (typical)	9.85	0.16	10 (k_θ) 1 (k_r)	... ...
Insulation (Mk II)	30	0.30	0.02	...

[a] $\eta = 0.5$, $hv_2 = 1000$ Btu/lb, $T_0 = 100$°F, $T_A = 2500$°F.

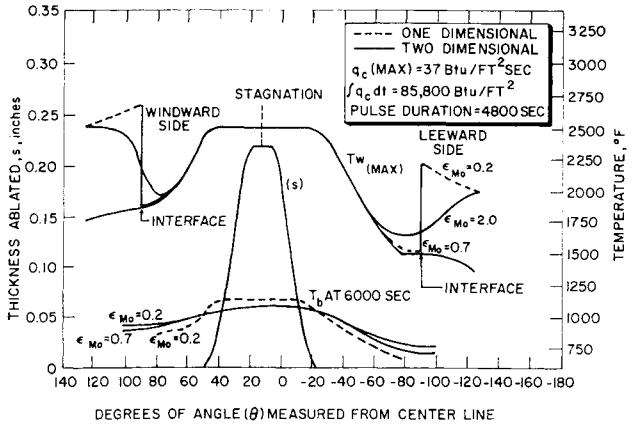

Fig. 4 Comparison of one- and two-dimensional analysis of temperature and ablation profiles in a wing leading edge, shown in Fig. 2.

may be treated in terms of its temperature limit and heat capacity, because no critical stress situation exists in either direction.

Ablation of a Spin Fin

A fin system for stabilizing an entry body in flight is a good example of a problem area requiring the determination of two- and possibly three-dimensional effects. If the fin is to provide both activation and timely inactivation of the system, the predictions of its recession-time and temperature-time histories become significant design criteria. Three modes of inactivation may be considered: 1) ultimately complete ablation, 2) structural failure because of aerodynamic loads, and 3) boundary-layer inactivation. For the first, mass loss and spin rate must be determined as functions of altitude. For the second, failure in bending (ultimate tensile stress) because of elevated temperature and loads may be used as a design criterion (or a more rigorous structural analysis may be carried out). For the third, the time-history ratio of fin characteristic dimension (base/apex height ratio) to boundary-layer thickness can be used with correlations[16, 17] between these parameters and spin induction. Of course, since the

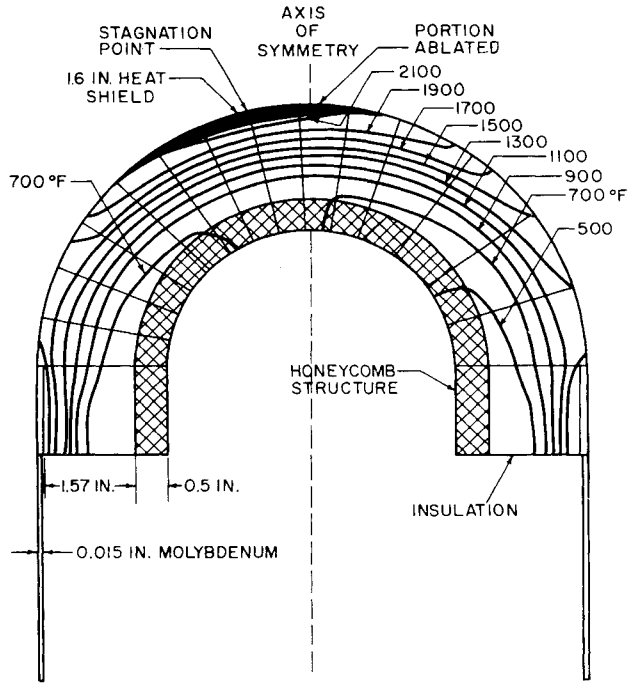

Fig. 5 Isotherms in a wing leading edge during re-entry (t = 4000 sec).

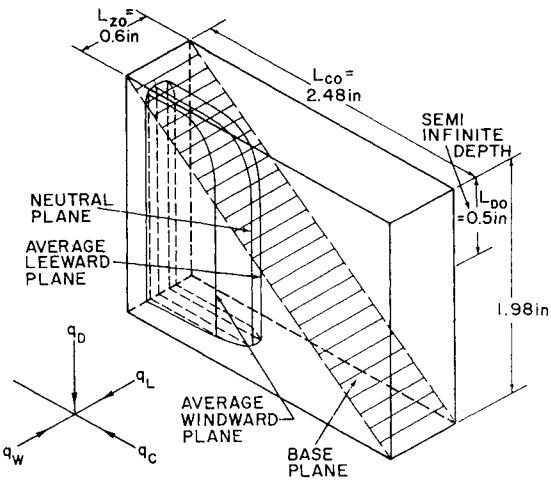

Fig. 6 Three-dimensional ablation profiles for spin fin.

time factor is a very sensitive parameter, a careful multidimensional analysis of ablation and heat flow is desirable.

The simple configuration considered (Fig. 6) is a rectangular slab subjected to heating on four faces: L leeward side, W windward side, C leading edge, and D top face. (The diagonal plane will be discussed later in the section on load failure.) The cold-wall heating is assumed to be spatially constant over each face and to have the same proportionate variation with time for each face (Fig. 7), within some constant factors. In Table 2, with the stagnation Q_C = 86,800 Btu/ft^2 as a reference, Q_L = 0.10 Q_C, Q_W = 0.15 Q_C, and Q_D = 0.125 Q_C. Another set of runs was made with the same Q_W, Q_L, and Q_D, but with the stagnation input reduced by $\frac{1}{2}$: Q_C' = 43,400 Btu/ft^2.

The boundary condition (3), satisfied at each of the faces, is given by

$$-k\frac{\partial T}{\partial n} = q_c\left(1 - \frac{h_w}{h_s}\right) - \epsilon\sigma T_w^4 - \rho s\{f_1\chi[h_{v_1} + \eta(h_s - h_w)] + (1 - \chi)[h_{v_2} + \eta(h_s - h_w)]\} \quad (28)$$

for the reinforced plastic. The vaporized fractions f_1 and the transpiration factors η used in this study are listed in Table 2, and material properties and ablation characteristics are given in Table 3.

Preliminary one-dimensional analyses[18, 19] had shown the need to treat the fin as a two- or three-dimensional body. However, the simultaneous accommodation of all heat inputs would require an inordinately large analog computer. The problem was therefore broken down into sets of one- and two-dimensional cases, the solutions of which were then synthesized on the computer to approximate three-dimensional behavior. The effect of shape change on the external flow and heating was not considered here but should be integrated into the final evaluation of the response.

Results are summarized in Table 4. First, four one-dimensional problems were constructed by considering each input separately as applied uniformly to a bar, the length of which corresponds to the thickness of the fin in that direction. It was thus determined that complete ablation occurs because of stagnation heating (corresponding to Q_C = 86,800 Btu/ft^2), and partial ablation because of the other inputs q_L, q_W, q_D. Specifically, 0.069 in. ablated in the leeward direction, 0.135 in. in the windward direction, and 0.112 in. from the top face. The continuous-recession analysis was not suitable for this application, because the transformation (10) does not allow for complete ablation (the denominator ($L_0 - s$) approaches zero); therefore, the stepwise method was used (total ablation introduces no singularities).

As a preliminary step toward obtaining three-dimensional results, a "neutral plane" was defined perpendicular to the

direction of two opposing heat inputs q_L and q_W, such that the heat flux across this plane was zero. Thus, the original geometrical configuration was replaced by a simpler one, with the neutral zero-flux plane as one of its boundaries. One-dimensional runs were made with only a single input (either q_L or q_W) introduced at one end of a bar of length (L_L or L_W) approximately one-half the initial thickness of the spin fin (L_{z0} = 0.6 in.), and the other end of the bar was assumed to be insulated. Lengths L_L and $L_W = L_{z0} - L_L$ for the leeward and windward bars were adjusted until each produced the same temperature history at the "insulated" end, which thus established the neutral plane. The neutral plane was found at L_L = 0.285 in.; hence L_W = 0.315 in. A two-dimensional model was established (Fig. 8) as follows: in one direction, the input was taken as the stagnation flux q_C (or q_C'), and in the other, q_L, q_W, or q_D, making a total of six cases. In essence, two cuts of the three-dimensonal fin (Fig. 6) were made: one horizontal slice with stagnation heating on one side, leeward or windward heating on the other, and the remaining two sides insulated; and a vertical slice, again with stagnation heating on one side, top heating on the other, and the remaining two sides insulated. For the leeward and windward inputs, the neutral plane established previously (L_L = 0.285 in.) was used. For the flux input from the top, the depth assumed was L_D = 0.5 in., since the one-dimensional calculations (case 1-D:4, Table 4) revealed that such a depth would be "semi-infinite" with respect to the shallow temperature penetration.

Table 2 Spin-fin heating

Side	Q_c-Btu/ft²	f_1	η
Leeward, L	8,680	0.9	0.25
Windward, W	13,020	0.9	0.25
Stagnation, C	86,800	0.14	0.70
Top, D	10,850	0.9	0.25

Table 3 Refrasil phenolic properties

ρ	= 81.0 lb/ft³	k_{char}	= 0.6 Btu/hr-ft-°F
c	= 0.2 Btu/lb-°F	ϵ_{char}	= 0.4
k	= 0.25 Btu/hr-ft-°F	T_A	= 4580°F
T_0	= 200°F	h_{v1}	= 5100 Btu/lb
T_{char}	= 1200°F	h_{v2}	= 1000 Btu/lb

Table 4 Ablation results for spin-fin re-entry

Case	Heat-flux direction	Slab thickness, L_0, in.	Ablated fraction, P	Ablation time, t_P or t_R, sec
One-Dimensional				
1	i:L	0.60	0.115	34.0
2	i:W	0.60	0.225	35.5
3	j:C	2.48	1.0	33.5
4	k:D	2.00	0.056	34.7
5	j:C'	2.48	0.5	36.5
Two-Dimensional				
6	j:C i:L	2.48 0.285	1.0	32.5
7	j:C i:W	2.48 0.315	1.0	32.0
8	j:C k:D	2.48 0.50	1.0	33.2
9	j:C' i:L	2.48 0.285	0.82	36.0
10	j:C' i:W	2.48 0.315	0.88	36.0
11	j:C' k:D	2.48 0.50	0.73	36.0
Three-Dimensional				
12	j:C, k:D; i:Neutral plane	2.48 0.50	1.0	32.0
13	j:C, k:D; i:L_{AV}	2.48 0.50	1.0	31.6
14	j:C, k:D; i:W_{AV}	2.48 0.50	1.0	31.5
15	j:C', k:D; i:Neutral plane	2.48 0.50	0.83	36.0
16	j:C', k:D; i:L_{AV}	2.48 0.50	0.83	36.0
17	j:C', k:D; i:W_{AV}	2.48 0.50	0.88	37.0

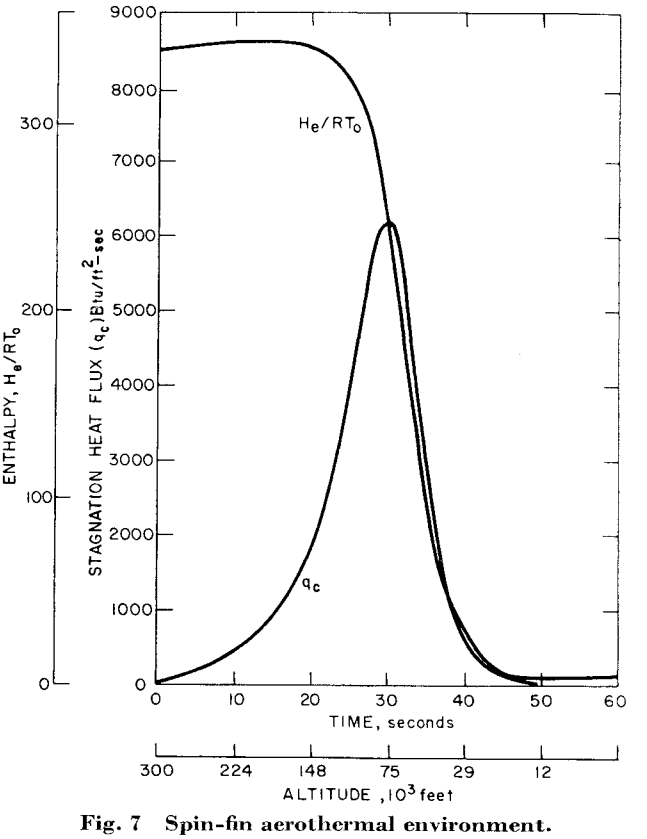

Fig. 7 Spin-fin aerothermal environment.

Results are shown in "sequential snapshots" in Fig. 8, which combines the two cases (2-D:6 and 2-D:7) of q_C with q_L and q_W. For the windward input, ablation is completed at the end of 32 sec, whereas for the smaller leeward input, 32.5 sec are required. (If the neutral plane had been specified exactly right, these two times would have been equal, between 32.0 and 32.5 sec.) Comparing this result with that for the one-dimensional case, where q_C was the sole input and total ablation required 33.5 sec, one sees that the one-dimensional solution underestimated the ablation time by 1.0 to 1.5 sec.

Typical two-dimensional ablation profiles (cases 2-D:9 and 10) at various times for Q_C' = 43,400 Btu/ft² are plotted in Fig. 9a and compared with those obtained by simple superposition of the three one-dimensional solutions (for q_C', q_L, q_W) in Fig. 9b. The effect of improper corner treatment in the superposition case can be observed, as well as the underestimate (~400°F) of the temperature response.

On the basis of these one- and two-dimensional results, th time for complete ablation was analyzed first. The initial volume of the rectangular slab was used as a reference basis for comparison of mass-loss computed by one- and two-dimensional simulation methods. Figure 10 shows the calculated mass-loss for each of the methods used. The one-dimensional curve is obtained by assuming that the rectangular volume ablates because of heating at the stagnation edge only; therefore, it recedes in a plane normal to the base plane.

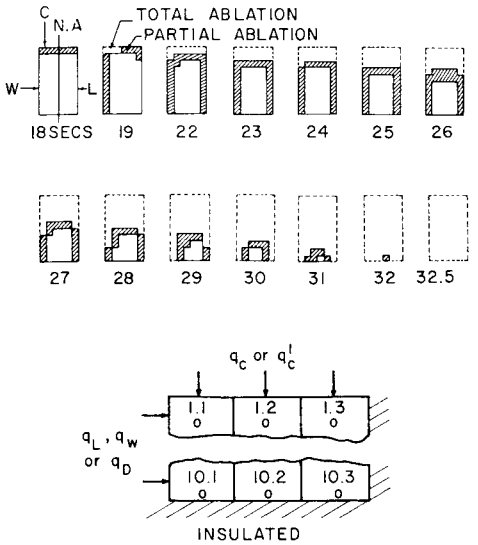

Fig. 8 Snapshot sequence of two-dimensional ablation (stagnation, windward, and leeward heating).

The two-dimensional curve is computed assuming heating in the C, L, and W directions, with no recession in the D direction, as in Fig. 9a, but with full stagnation heating. The superposition curve corresponds similarly to Fig. 9b. It is clear that the two-dimensional method predicts higher ablation rates, with a significant reduction in the time of removal.

The next step in the analysis was to obtain approximate three-dimensional results as follows. Three vertical slices of the given solid were formed: one at the neutral plane, one at an "average" leeward plane, and one at an "average" windward plane. The two average planes were taken approximately midway between the neutral plane and the outer surfaces. Each of the three slices was subjected, in turn, to heating from the stagnation direction (q_C or q_C') and from the top (q_D). The three-dimensional effect was then simulated in each of the three cases by introducing at each of 30 stations in the vertical slice an equivalent flux obtained for that particular plane from the one-dimensional analysis of the bar subjected to q_L and q_W. It is reasoned that this approach yields an upper bound for the recession rates of the three vertical slices, because the inserted horizontal fluxes were greater than those that would actually exist, due to the fact that, in the one-dimensional horizontal calculations, the temperatures of interior points were unaffected by vertical heating and were, therefore, unrealistically low; hence, the horizontal fluxes were unrealistically high.

Total ablation of the neutral plane occurred in 32 sec, of the average leeward plane in 31.6 sec, and of the average windward plane in 31.5 sec. Recapitulating, one-dimensional analysis gave 33.5 sec, and two-dimensional analysis gave 32+ sec. This quasi-three-dimensional analysis decreased the ablation time by another $\frac{1}{2}$ sec or more, but the latter result is likely to be on the low side, for the reason discussed previously. The true answer, therefore, within the framework of the assumptions, is $32.5 > t > 31.5$ sec, which represents a correction of approximately $1\frac{1}{2}$ sec compared to the one-dimensional results. A three-dimensional ablation profile is shown in Fig. 6 for the stagnation flux q_C', based on the individual curves obtained for the three vertical planes.

The second mode of failure considered was that due to loads at elevated temperatures. The one-dimensional calculation indicates very shallow thermal penetration behind the ablation front; thus no significant departure from a failure due solely to ablation could be expected. On the other hand, two-dimensional calculations indicate significant penetration of the isotherms and suggest possible failure prior to that indicated by the mass-removal criterion. The diagonal cross section of the rectangular volume (Fig. 6) could be considered

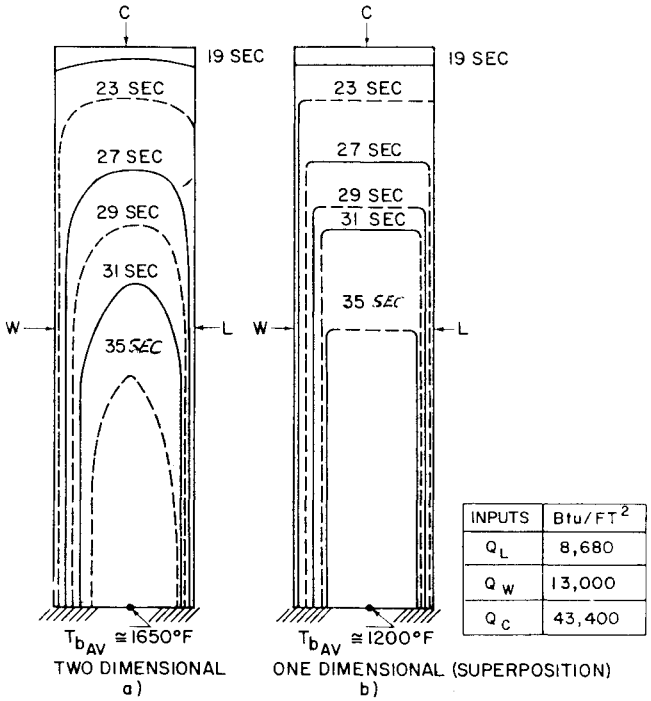

Fig. 9 One- and two-dimensional ablation profiles in refrasil phenolic.

representative of a typical fin base area (maximum stress). The ratio of an area remaining below a given temperature level to this initial reference base area was calculated as a function of time for the one-dimensional, superposition, and two-dimensional methods. Actual stress calculations are beyond the scope of this paper, and, for lack of a well-established failure criterion, no exact determination of the failure time can be given. If a given area ratio could be taken as a failure criterion corresponding to a given stress distribution, the three computational methods could be compared, as in Fig. 11. Given the insensitivity of one-dimensional results to the temperature level, truly two-dimensional calculations would indicate earlier failure times than the one-dimensional case. Superposition results tend to improve the one-dimensional predictions somewhat.

The importance of accurate calculation of time of fin removal can be demonstrated by comparing the results in Figs. 10 and 11 with computed relative dispersions (miss distances) as functions of altitude at which control ceased. If one considers the one-dimensional estimate of ablation failure altitude, 56,000 ft (Fig. 10), as reference and then computes the relative dispersion ($\partial D/\partial D_{ref}$) for the two-dimensional failure altitude of 67,000 ft, a factor of $\sim$6 is obtained. Similarly, using a given area ratio from Fig. 11 as a criterion, it follows that a corresponding error factor in the dispersion would be $\gg$10.

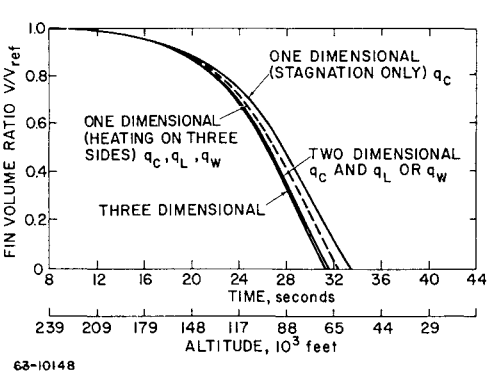

Fig. 10 Comparison of methods based on spin-fin ablation.

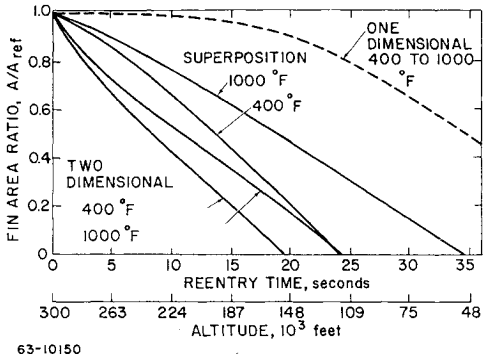

Fig. 11 Comparison of methods using base temperature.

Concluding Remarks

1) Discrete stepwise ablation and continuous recession constitute two methods for the practical solution on an analog computer of multidimensional ablation and heat-flow problems. These treatments afford analyses of those problems for which a strictly one-dimensional approach may not suffice.

2) For the wing leading edge, the two-dimensional analysis (compared to one-dimensional) showed lower base temperatures (50°–70°F reduction on ~1100°F) and much smoother profiles at the plastic-to-molybdenum skin juncture.

3) For the ablated spin-control fin, comparisons showed that one-dimensional analysis underestimated the ablation failure by ~1½ sec (on 32). For earlier failures based on stresses on the reduced sections at elevated temperatures, the two-dimensional solutions indicate failures at much higher altitudes, which could lead to increases in vehicle dispersion of one or more orders of magnitude.

References

[1] Hurwicz, H. and Collins, J. A., "Thermal analysis of the shape 52 ICBM re-entry vehicle," Avco RAD-TR-9-59-10 (March 1959).

[2] Beck, J., "Axisymmetric transient heat conduction in a rocket nozzle calorimeter," Avco RAD-7 (VIII)-TM-60-6 (April 1960).

[3] Wolf, H., "A program analysis for two-dimensional heat flow," Avco RAD-9-TM-59-1 (February 1959).

[4] Baylor, R. N. and Conrey, C. L., "The calculation of the effects of internal cross radiation on transient temperature distributions in hypersonic vehicles," Chance-Vought Rept. E9R-12456 (October 1959).

[5] Fleddermann, R. G. and Hurwicz, H., "Analysis of transient ablation and heat conduction phenomena at a vaporizing surface," Chem. Eng. Prog. Symp. Ser. **57** (32) 24 (1960); also Avco RAD-TR-9 (7)-60-9 (April 1960).

[6] Hurwicz, H. and Fleddermann, R. G., "Computer simulation of transient ablation and heat conduction phenomena at a vaporizing surface," ARS Preprint 2209-61 (1961).

[7] Zlotnick, M. and Nordquist, B., "Calculation of transient ablation," International Development Heat Transfer Conference, ASME, Boulder, Colo. (September 1961), pp. 725–731.

[8] Adams, E. W., "Analysis of quartz and teflon shields for a particular re-entry mission," Proc. 1961 Heat Transfer and Fluid Mech. Inst., Pasadena, Calif. (June 1961).

[9] Nolan, E. J. and Scala, S. M., "The aerothermodynamic behavior of pyrolytic graphite during sustained hypersonic flight," ARS Preprint 1696–61 (April 1961).

[10] Hurwicz, H. and Mascola, R. E., "Thermal protection system—applications research of material properties and structural concepts," Aeronaut. Systems Div., ASD-TDR-62-656 (July 1962).

[11] Hurwicz, H., "Aerothermochemistry studies in ablation," *Combustion and Propulsion: Fifth AGARD Colloquium* (Pergamon Press, Oxford, England, 1963), pp. 403–455.

[12] Fifer, S., *Analogue Computation* (McGraw-Hill Book Co., Inc., New York, 1961), Vols. I–IV.

[13] Carslaw, H. S. and Jaeger, J. C., *Conduction of Heat Solids* (Clarendon Press, Oxford, England, 1959), 2nd ed., Chap. 1.

[14] Landau, H. H., "Heat conduction in melting solids," Quart. J. Mech. Appl. Math. **8**, 81 (1950).

[15] Dian Laboratories, Inc., private communication, Avco RAD (1957).

[16] James, R. W. and Hill, F. J. J., Jr., Avco RAD, private communications (August 1961).

[17] Sellers, R. B., Avco RAD, private communications (October 1960).

[18] Campbell, W. F., "A rapid analytical method for calculating the early transient temperature in a composite slab," National Research Lab. Rept. 32 (April 1956).

[19] Forsythe, G. and Wasow, W., *Finite Difference Methods for Partial Differential Equations* (John Wiley and Sons, Inc., New York, 1960).